Condensation of Pyramidal $[AsSe_3]^{3-}$ Anions for the Construction of Polymeric Networks: Solventothermal Synthesis of $K_3AgAs_2Se_5 \cdot 0.25MeOH$, $K_2AgAs_3Se_6$, and $Rb_2AgAs_3Se_6$

M. Wachhold and M. G. Kanatzidis*

Department of Chemistry and Center for Fundamental Materials Research, Michigan State University, East Lansing, Michigan 48824

Received March 8, 1999

Three novel quaternary selenoarsenates could be synthesized by the solventothermal reaction of $[AsSe_3]^{3-}$ anions with $AgBF_4$ in the presence of the respective alkali metal cation. Orange crystals of $K_3AgAs_2Se_5 \cdot 0.25MeOH$ (**I**) are formed after reaction in MeOH at 130 °C for ∼2 h. Its structure is built up of ψ-bitetrahedral $[As_2Se_5]^{4-}$ units, which are connected by Ag^+ ions to form anionic one-dimensional chains. These chains are separated from each other by the K^+ cations. Longer reaction time, i.e., 3 days, at the same temperature provides red crystals of $K_2AgAs_3Se_6$ (**II**) and, correspondingly, the isostructural $Rb_2AgAs_3Se_6$ (**III**), which possess two-dimensional (2D) polyanions $[AgAs_3Se_6]^{2-}$. They consist of double layers of strongly waved, infinite $[AsSe_2]^-$ chains, which are interconnected by tetrahedral Ag^+ ions. The structure can also be described as $[Ag_2As_6Se_{14}]^{8-}$ cores, which are connected by bridging Se atoms to build the sheet anion. Both **II** and **III** possess Ag_2Se_2 four-membered rings, which lead to Ag···Ag distances between 3 and 3.3 Å. The thermal, optical, and spectroscopic properties of the compounds are reported. They melt incongruently between 259 and 284 °C and are wide band gap semiconductors with values between 1.9 and 2.1 eV. Raman spectroscopic data show typical patterns for the respective selenoarsenate anionic building units in the range 100−300 cm^{-1}. Crystal data: $K_3AgAs_2Se_5 \cdot 0.25MeOH$ (**I**), monoclinic, $P2_1/c$, $a = 9.229(1)$ Å, $b = 11.508(2)$ Å, $c = 12.905(2)$ Å, $\beta = 104.272(2)°$, $Z = 4$; $K_2AgAs_3Se_6$ (**II**), monoclinic, $P2_1/n$, $a = 12.5994(6)$ Å, $b = 7.4980(4)$ Å, $c = 14.2648(7)$ Å, $\beta = 96.625(2)°$, $Z = 4$; $Rb_2AgAs_3Se_6$ (**III**), monoclinic, $P2_1/n$, $a = 12.717(2)$ Å, $b = 7.7329(8)$ Å, $c = 14.368(2)$ Å, $\beta = 95.745(2)°$, $Z = 4$.

Introduction

In recent years, solventothermal and molten salt synthesis techniques proved to be a powerful method for access to a huge number of new binary, ternary, and quaternary chalcogenido compounds.[1,2] The dimensionality of the anionic parts of the structures varies hereby from isolated building blocks to infinite frameworks. A structure-directing effect of the cations, such as alkali metals or quaternary ammonium or phosphonium salts, is well recognized for a number of examples.[3] There exists a clear correlation where smaller cations stabilize higher dimensional structures and favor higher coordination numbers in a framework of a given composition. Salutary examples with a number of comparable compounds are the Cu/Ag polychalcogenides $(Ph_4P)[Ag(Se_4)]$,[4] $(Me_4N)[Ag(Se_5)]$,[5] α-$KCuS_4$,[6a] $CsCuS_6$,[6b] $[(Et_4N)Ag(Se_4)]_4$,[7] and $(Me_4N)[Ag(Te_4)]$[8] or the Pd polyselenides K_2PdSe_{10},[9] Rb_2PdSe_{16},[10] Cs_2PdSe_8,[11] $[(H_3C)N(CH_2CH_2)_3N(CH_3)][Pd(Se_6)_2]$,[12] $(H_3NCH_2CH_2NH_2)_2[Pd(Se_5)_2]$,[12] $K_2[(H_3NCH_2CH_2NH_3)_2][Pd(Se_4)_2 \cdot 2Se_4]$,[12] $(NEt_4)_5[Pd(Se_4)_2 \cdot 0.5Pd(Se_5)_2]$,[13] and $(Ph_4P)_2[Pd(Se_4)_2]$.[14] Both groups of compounds clearly illustrate the role of the countercation size and shape in stabilizing molecular vs extended structures of variable dimensionalities.[2,7,12]

In the particular case of solventothermal synthesis of ternary or quaternary group 15/16 compounds, the ability of the pyramidal $[MQ_3]^{3-}$ anions (M = As, Sb; Q = S, Se) to undergo a variety of condensation and ring closure reactions has opened access to a large number of new compounds with novel anionic building units. Occasionally this anion itself can be part of an anionic structure; e.g., $[AsSe_3]^{3-}$ anions are present in $(R_4N)[HgAsSe_3]$ (R = Me, Et)[15] or $[SbQ_3]^{3-}$ anions are present in

(1) (a) Sheldrick, W. S.; Wachhold, M. *Coord. Chem. Rev.* **1998**, *176*, 211. (b) Sheldrick, W. S.; Wachhold, M. *Angew. Chem., Int. Ed. Engl.* **1997**, *36*, 206. (c) Drake, G. W.; Kolis, J. W. *Coord. Chem. Rev.* **1994**, *137*, 131. (d) Roof, L. C.; Kolis, J. W. *Chem. Rev.* **1993**, *93*, 1037. (e) Liao, J.-H.; Kanatzidis, M. G. *J. Am. Chem. Soc.* **1990**, *112*, 7400−7402. (f) Liao, J.-H.; Kanatzidis, M. G. *Inorg. Chem.* **1992**, *31*, 431−439. (g) Kanatzidis, M. G.; Das, B. K. *Comments Inorg. Chem.* **1999**, *21*, 29−51.

(2) (a) Kanatzidis, M. G.; Sutorik, A. C. *Prog. Inorg. Chem.* **1995**, *43*, 151. (b) Kanatzidis, M. G.; Huang, S.-P. *Coord. Chem. Rev.* **1994**, *130*, 509. (c) Kanatzidis, M. G. *Curr. Opin. Solid State Mater. Sci.* **1997**, *2*, 139.

(3) Kanatzidis, M. G. *Phosphorus, Sulfur Silicon Relat. Elem.* **1994**, *93*−*94*, 159.

(4) Kanatzidis, M. G.; Huang, S.-P. *J. Am. Chem. Soc.* **1989**, *111*, 760.

(5) Banda, R. M. H.; Craig, D. C.; Dance, I. G.; Scudder, M. L. *Polyhedron* **1989**, *8*, 2379.

(6) (a) Kanatzidis, M. G.; Park, Y. *J. Am. Chem. Soc.* **1989**, *111*, 3767. (b) McCarthy, T. J.; Zhang, X.; Kanatzidis, M. G. *Inorg. Chem.* **1993**, *32*, 2944.

(7) Huang, S.-P.; Kanatzidis, M. G. *Inorg. Chem.* **1991**, *30*, 1455.

(8) Kim, K.-W.; Kanatzidis, M. G. *J. Am. Chem. Soc.* **1993**, *115*, 5871.

(9) Kim, K.-W.; Kanatzidis, M. G. *J. Am. Chem. Soc.* **1992**, *114*, 4878.

(10) Kanatzidis, M. G.; Wachhold, M. *J. Am. Chem. Soc.* **1999**, *121*, 4189.

(11) Li, J.; Chen, Z.; Wang, R.-J.; Lu, J. Y. *J. Solid State Chem.* **1998**, *140*, 149.

(12) Kim, K.-W.; Kanatzidis, M. G. *J. Am. Chem. Soc.* **1998**, *120*, 8124.

(13) McConnachie, J. M.; Ansari, M. A.; Ibers, J. A. *Inorg. Chem.* **1993**, *32*, 3250.

(14) (a) Kräuter, G.; Dehnicke, K. *Chem. Ztg.* **1990**, *114*, 7. (b) Adams, R. D.; Wolfe, T. A.; Eichhorn, B. W.; Haushalter, R. C. *Polyhedron* **1989**, *8*, 701. (c) Kim, K.-W.; Kanatzidis, M. G. *Inorg. Chem.* **1993**, *32*, 4161.

(15) Chou, J.-H.; Kanatzidis, M. G. *J. Solid State Chem.* **1996**, *123*, 115.

10.1021/ic990274r CCC: $18.00
Published on Web 08/05/1999

$Na_2[CuSbS_3]$[16] and $Cu_2SbSe_3 \cdot x$en ($x = 0.5$, 1; en = ethylenediamine).[17] Whereas $[AsSe_3]^{3-}$ was used as a reactant (in the form of an alkali metal salt) for the first compound, the anion in the latter two was generated from other reactants. The most powerful characteristic feature of the $[MQ_3]^{3-}$ anion, however, is its ability to undergo various types of condensation reactions, such as oligomeric chain or ring formation, until a building block is created capable to "fit" in the crystal lattice under the given reaction conditions. This property to self-condense is particularly useful for the synthesis of quaternary compounds.

Stepwise condensation reactions of the $[AsQ_3]^{3-}$ anion (Q = S, Se) such as

$$[AsQ_3]^{3-} + [AsQ_3]^{3-} \rightarrow [As_2Q_5]^{4-} + Q^{2-} \quad (1)$$

$$[As_2Q_5]^{4-} + [AsQ_3]^{3-} \rightarrow [As_3Q_7]^{5-} + Q^{2-} \quad (2)$$

$$[As_3Q_7]^{5-} + [AsQ_3]^{3-} \rightarrow [As_4Q_9]^{6-} + Q^{2-} \quad (3)$$

led to several novel compounds such as $(R_4N)[Mo_2O_2Q_2(As_2Q_5)]$ (R = Me, Q = S; R = Et, E = Se),[18] $(Me_3NH)[Ag_3As_2Se_5]$, $K_5[Ag_2(AsSe_4)(As_2Se_5)]$,[19] $(Ph_4P)[InAs_3S_7]$,[20] and $K_2[Ag_6(AsS_3)(As_3S_7)]$,[19] $(Ph_4P)_2[Hg_2As_4S_9]$[21] with various oligomeric $[As_xQ_{2x+1}]^{(2+x)-}$ chain anions. Ring closure reactions such as

$$[As_3S_7]^{5-} \rightarrow [As_3S_6]^{3-} + S^{2-} \quad (4)$$

$$[As_4S_9]^{6-} \rightarrow [As_4S_8]^{4-} + S^{2-} \quad (5)$$

led to anions that are present in $(Me_4N)_2Rb[Bi(As_3S_6)_2]$[20] and $(Ph_4P)_2[NiAs_4S_8]$.[18] Undoubtedly these reactions are facilitated if not enabled by protonation in solution. The protons are supplied by the alcohol or H_2O. In contrast, solventothermal reactions carried out in the aprotic solvent ethylenediamine (en) predominantly produce compounds with simple units such as $[MS_3]^{3-}$ or $[MS_4]^{3-}$ (M = As, Sb). Condensed $[M_xQ_y]^{n-}$ units are rarely observed.[17,22,26,28] The $[As_3S_6]^{3-}$ six-membered ring with chair conformation or its higher homologue $[As_3Se_6]^{3-}$ is well-known as a discrete molecular anion in a number of compounds.[23] The condensation of the two central As atoms in $[As_4S_9]^{6-}$ leads to a four-membered As_2S_2 ring in the $[As_4S_8]^{4-}$ anion. The formation of $(Me_4N)_2Rb[Bi(As_3S_6)_2]$ shows that it can be very useful to provide two differently sized cations in the reaction solution, since in some cases special adaptations seem to be necessary to stabilize certain structure types.

Infinite condensation of $[MQ_3]^{3-}$ units leads to the $[MQ_2^-]_n$ chain in $[Co(en)_3][CoSb_4S_8]$,[24] well-known from a number of other ternary and quaternary compounds such as $AAsSe_2$ (A = K, Rb, Cs)[25] and $Cs_3[Ag_2(SbS_2)_2(SbS_4)]$.[26]

$$n[MQ_3]^{3-} \rightarrow [MQ_2^-]_n + nQ^{2-} \quad (6)$$

An interesting branched isomer $[As_3S_6^{3-}]$ of the simple chain is present in $(Me_4N)[HgAs_3S_6]$;[21] every second As ribbon atom carries a side chain AsS_3 unit instead of a terminal S atom. When the Q^{2-} anion in $[MQ_3]^{3-}$ is exchanged by a Q_2^{2-} dumbbell, an $[MQ_4]^{3-}$ anion is created, which also can act as a coordinating ligand, as for example in $(Ph_4P)_2K(Pt_3(AsS_4)_3]\cdot 1.5H_2O$.[27] Combination of both condensation and substitution steps led also to unusual anions such as $[As_4Se_{11}]^{6-}$ in $(Ph_4P)[Hg_2As_4Se_{11}]$,[14] which is a formal product of reactions 1−3, followed by a substitution of one terminal Se atom on each of the outer As atoms of the $[As_4Se_9]^{6-}$ anion; see eq 7.

$$[As_4Se_9]^{6-} + 2Se_2^{2-} \rightarrow [As_4Se_{11}]^{6-} + 2Se^{2-} \quad (7)$$

Compared with the structural variety of M_xQ_y anions containing an As^{3+} or Sb^{3+} center, the structures of M^{5+} compounds is so far limited to the tetrahedral $[MQ_4]^{3-}$ anion (a structural isomer of the one mentioned above). For example, several phases of the general composition $A_{2-x}Ag_xMS_4$ ($x = 1$, 2; A = K, Rb, Cs; M = As, Sb) could be synthesized by Kolis and co-workers.[26,28] In $K_5[Ag_2(AsSe_4)(As_2Se_5)]$[19] and $Cs_3[Ag_2(SbS_2)_2(SbS_4)]$,[26] these anions are also part of the polyanion structure.

Here we report the synthesis, structural characterization, and properties of three new silver selenoarsenates with strongly related anionic structures, namely $K_3AgAs_2Se_5\cdot 0.25$MeOH (**I**), $K_2AgAs_3Se_6$ (**II**), and $Rb_2AgAs_3Se_6$ (**III**). The last two compounds are isostructural and reveal sheet anions with $[AsSe_2]^-$ undulated chains connected by tetrahedral coordinated Ag^+ atoms. The resulting $[AgAs_3Se_6]^{2-}$ sheets contain huge holes, which are able to accommodate the alkali metal cations and therefore show close van der Waals contacts to each other. $K_3AgAs_2Se_5\cdot 0.25$MeOH is a "trapped" intermediate on the way to the formation of $K_2AgAs_3Se_6$.

Experimental Section

Reagents. Chemicals were used as obtained without further purification: Rb_2CO_3, $AgBF_4$, methanol (99.9%), J. T. Baker; diethyl ether (>99.0%), CCI. All experiments and manipulations were performed under an atmosphere of dry nitrogen using a vacuum atmosphere Dri-Lab glovebox.

Syntheses. Li_2Se and K_2Se. Li_2Se and K_2Se were prepared by reaction of stoichiometric amounts of potassium or lithium metal and black selenium in liquid ammonia.[29]

Li_3AsSe_3. Li_2Se and As_2Se_3 were ground thoroughly and mixed in a 1:3 ratio to load into a quartz tube (o.d. 13 mm). The tube was sealed under high vacuum ($\sim 10^{-4}$ mbar) and then heated to 300 °C in 10 h and subsequently to 450 °C in 96 h and isothermed at this temperature for 100 h. After the mixture was cooled to room temperature (100 h), dark-brown Li_3AsSe_3 was isolated and ground to a powder. The X-ray diffraction powder pattern indicates that this phase is not isostructural with the corresponding Na^+ and K^+ phases (see below).

K_3AsSe_3. K_2Se and As_2Se_3 were ground thoroughly, mixed in a 1:3 ratio, and loaded into a quartz tube. The tube was sealed under high vacuum ($\sim 10^{-4}$ mbar) and then heated to 300 °C in 10 h and subsequently to 450 °C in 72 h and isothermed at this temperature for 100 h. After cooling (10 h), the brown-orange K_3AsSe_3 was isolated and ground to a powder. The X-ray diffraction powder pattern shows

(16) Jerome, J. E.; Schimek, G. L.; Drake, G. W.; Kolis, J. W. *Eur. J. Solid State Inorg. Chem.* **1996**, *33*, 765.
(17) Chen, Z.; Dilks, R. E.; Wang, R.-J.; Lu, J. Y.; Li, J. *Chem. Mater.* **1998**, *10*, 3184.
(18) Chou, J.-H.; Hanko, J. A.; Kanatzidis, M. G. *Inorg. Chem.* **1997**, *36*, 4.
(19) Kanatzidis, M. G.; Chou, J.-H. *J. Solid State Chem.* **1996**, *127*, 186.
(20) Chou, J.-H.; Kanatzidis, M. G. *Inorg. Chem.* **1994**, *33*, 1001.
(21) Chou, J.-H.; Kanatzidis, M. G. *Chem. Mater.* **1995**, *7*, 5.
(22) Jerome, J. E.; Wood, P. T.; Pennington, W. T.; Kolis, J. W. *Inorg. Chem.* **1994**, *33*, 1733.
(23) (a) Sheldrick, W. S.; Kaub, J. *Z. Naturforsch., B* **1985**, *40*, 19. (b) Sheldrick, W. S.; Kaub, J. *Z. Naturforsch., B* **1985**, *40*, 1020.
(24) Stephan, H.-O.; Kanatzidis, M. G. *J. Am. Chem. Soc.* **1996**, *118*, 12226.
(25) Sheldrick, W. S.; Häusler, H.-J. *Z. Anorg. Allg. Chem.* **1988**, *561*, 139.
(26) Wood, P. T.; Schimek, G. L.; Kolis, J. W. *Chem. Mater.* **1996**, *8*, 721.
(27) Chou, J.-H.; Kanatzidis, M. G. *Inorg. Chem.* **1994**, *33*, 5372.
(28) (a) Schimek, G. L.; Kolis, J. W. *Acta Crystallogr., Sect. C* **1997**, *53*, 991. (b) Schimek, G. L.; Pennington, W. T.; Wood, P. T.; Kolis, J. W. *J. Solid State Chem.* **1996**, *123*, 277.
(29) Fehér, F. In *Handbuch der präparativen Anorganischen Chemie*; Brauer, G., Ed.; Ferdinand Enke Verlag: Stuttgart, Germany, 1975; Vol. 1, p 372f.

that it is isostructural with the recently published A_3AsSe_3 (A = Na, K) phases,[30] which possess, among others,[31] the Na_3AsS_3 structure type.[32]

$K_3AgAs_2Se_5$·0.25MeOH. This compound was synthesized by the reaction of 0.020 g (0.1 mmol) of $AgBF_4$ and 0.129 g (0.3 mmol) of K_3AsSe_3 in 1 mL of MeOH. The starting materials were mixed thoroughly, loaded into a Pyrex tube (o.d. 13 mm, ~10 cm^3 volume), and sealed under vacuum. The tube was kept at 130 °C for 2 h. After the product was washed with MeOH, water, and diethyl ether, orange, cubic-shaped crystals were obtained as the main product, together with some very small, dark-red, polyhedral crystals (altogether 35% yield based on Ag). Semiquantitative analysis by the SEM/EDS technique on the orange crystals gave $K_{2.4}Ag_1As_{1.7}Se_{3.4}$, with the red crystals showing a very similar stoichiometry. The purity of the compound was confirmed by comparison of the powder X-ray diffraction pattern of the homogenized and ground material with the one calculated from single-crystal X-ray data.[33] The X-ray diffraction pattern proves the presence of a second phase: the diffraction region of $2\theta < 15°$ shows a strong reflection at $d = 8.64$ Å and a weaker one at $d = 9.2$ Å, which both belong to $K_3AgAs_2Se_5$·0.25MeOH; a weak reflection at $d = 10.6$ Å, however, could not be assigned to this or any other known binary, ternary, or quaternary compound and is therefore most probably caused by a second new phase. The ratio of these two compounds was approximately 90:10, according to the highest peak intensities. We also tried to identify this minor phase by single-crystal X-ray data collection, but due to the very small crystal size and poor crystallinity, we were not successful.

$K_2AgAs_3Se_6$. This compound was synthesized by the reaction of 0.020 g (0.1 mmol) of $AgBF_4$ and 0.129 g (0.3 mmol) of K_3AsSe_3 in 1 mL of MeOH. The starting materials were sealed under vacuum in a Pyrex tube and kept at 130 °C for 72 h. Small, leaf-shaped, dark-red crystals were obtained, together with black crystals of $K_5Ag_2As_3Se_9$[20] as a minor phase (typical yield 40−50% on Ag). The compound was washed with MeOH, water, and diethyl ether. Semiquantitative microprobe analysis on single crystals gave the stoichiometry as $K_2Ag_{0.79}As_{2.86}Se_{7.78}$. The powder X-ray diffraction pattern of the homogenized and ground material showed that, besides $K_5Ag_2As_3Se_9$, some elemental Se is present as an impurity.

$Rb_2AgAs_3Se_6$. A 0.024 g (0.2 mmol) sample of RbCl, 0.020 g (0.1 mmol) of $AgBF_4$, and 0.100 g (0.3 mmol) of Li_3AsSe_3 were mixed thoroughly and loaded into a Pyrex tube, together with 1.0 mL of MeOH. After sealing, the tube was heated at 140 °C for 70 h. Dark-red, polyhedral crystals of the product were grown (yield 75%), which were washed with water and diethyl ether. Semiquantitative microprobe analysis on single crystals confirmed the presence of a quaternary phase with an elemental composition of $Rb_2Ag_{0.63}As_{2.76}Se_{3.48}$. The powder X-ray diffraction pattern of the homogenized and ground material confirmed the purity of the obtained phase.

Physicochemical Methods. Solid State UV/Vis Spectroscopy. Single-crystal UV/vis spectra were recorded at room temperature on a computer-controlled Hitachi FT U6000 spectrometer associated with an Olympus BH2-UMA microscope in the wavelength range 380/900 nm. UV−vis−near-IR diffuse reflectance spectra of bulk powder samples were obtained on a Shimadzu UV-3101PC double-beam, double-monochromator spectrophotometer in the wavelength range 200−2500 nm. $BaSO_4$ powder was used as a reference (100% reflectance) and base material, on which the ground powder sample was coated. Reflectance data were converted to absorbance data as described elsewhere.[34] The band gap energy value was determined by extrapolation from the linear portion of the absorption edge in a (α/S) versus energy plot.

Differential Thermal Analysis (DTA) and Thermal Gravimetric Analysis (TGA). DTA experiments were performed on a computer-controlled Shimadzu DTA-50 thermal analyzer. Typically, 15−20 mg of ground material was sealed in a carbon-coated quartz ampule under vacuum. A sealed quartz ampule of equal mass filled with Al_2O_3 was used as a reference. The sample was heated to the desired temperature at 5 °C/min and isothermed for 1 min, followed by cooling at −5 °C/min to 50 °C. The sample stability was monitored by running a second heating/cooling cycle. The residues were examined by X-ray powder diffraction. The TGA analysis of **I** was performed on a computer-controlled Shimadzu TGA-50 thermal analyzer. 4 mg of the sample was charged into a quartz bucket and heated to 500 °C at a rate of 10 °C/min under a steady flow of dry N_2 gas.

Raman Spectroscopy. Raman spectra of suitable crystals with a clean surface were recorded on a Holoprobe Raman spectrograph equipped with a 633 nm helium−neon laser and a CCD camera detector. The instrument was coupled to an Olympus BX60 microscope. The spot size of the laser beam was 10 mm when a 50× objective lens was used.

Semiquantitative Microprobe Analysis. The analyses were performed using a JEOL JSM-35C scanning electron microscope (SEM) equipped with a Tracor Northern energy dispersive spectroscopy (EDS) detector. Data were acquired on several crystals using a 20 kV accelerating voltage and 30−35 s accumulation time.

X-ray Crystallography. Single crystals of the three compounds (crystal sizes: **I** 0.30 × 0.30 × 0.25, **II** 0.22 × 0.11 × 0.01, **III** 0.08 × 0.06 × 0.05) were sealed in glass capillaries (o.d. 0.3 mm, wall thickness $^1/_{100}$ mm) and mounted on a goniometer head. Crystallographic data sets for all three compound were collected on a Siemens Platform CCD diffractometer using graphite-monochromatized Mo Kα radiation. The data were collected over a full sphere of reciprocal space, up to 54−58° in 2θ. The individual frames were measured with an ω rotation of 0.3° and acquisition times of 30−45 s. SMART[35] software was used for the data acquisition, and SAINT[36] was used for data extraction and reduction. The absorption correction was performed using SADABS.[37]

Structure solutions and refinements were performed with the SHELXTL package of crystallographic programs.[38] All three structures were solved in monoclinic space groups, i.e., $P2_1/c$ for $K_3AgSe_2Se_5$·0.25MeOH and $P2_1/n$ for $K_2AgAs_3Se_6$ and $Rb_2AgAs_3Se_6$. All non-hydrogen atoms, except the C and O atoms of **I**, were refined anisotropically. Since the rest electron density gave evidence of a not fully occupied C,O position, their occupation factor was also refined.[39] Complete data collection parameters and details of the structure solution and refinement for **I**−**III** are given in Table 1. Fractional atomic coordinates and equivalent isotropic displacement parameters (U_{eq}) are given in Table 2, and bond parameters are given in Table 3.

Results and Discussion

Synthesis. The reaction of $AgBF_4$ with K_3AsSe_3 in MeOH at 130 °C provides two new quaternary silver selenoarsenates with new anionic structures. Their formation is strongly dependent on the reaction time. If the reaction is stopped after ca. 2 h, $K_3AgAs_2Se_5$·0.25MeOH (**I**) is formed; a longer reaction time of 3−4 days, on the other hand, leads to $K_2AgAs_3Se_6$ (**II**) as the main product, together with the known phase $K_5Ag_2As_3Se_9$.[19] If Li_3AsSe_3 is used instead of K_3AsSe_3, we have the possibility to provide other desired cations as counterions, since

(30) Bronger, W.; Donike, A.; Schmitz, D. *Z. Anorg. Allg. Chem.* **1998**, *624*, 553.
(31) See, for example: (a) Bronger, W.; Donike, A.; Schmitz, D. *Z. Anorg. Allg. Chem.* **1996**, *622*, 1003. (b) Lin, J.; Miller, G. J. *J. Solid State Chem.* **1994**, *113*, 296.
(32) (a) Hoppe, R.; Sommer, H. *Z. Anorg. Allg. Chem.* **1977**, *430*, 199. (b) Palazzi, M. *Acta Crystallogr., Sect. B* **1976**, *32*, 2175.
(33) *CERIUS*^{2}, Version 2.35; Molecular Simulations Inc.: Cambridge, U.K., 1995.
(34) Zhang, X.; Kanatzidis, M. G. *J. Am. Chem. Soc.* **1994**, *116*, 1890.
(35) *SMART*, Version 5; Siemens Analytical X-ray Systems, Inc.: Madison, WI, 1998.
(36) *SAINT*, Version 4; Siemens Analytical X-ray Systems, Inc.: Madison, WI, 1994−1996.
(37) Sheldrick, G. M. *SADABS*; University of Göttingen: Göttingen, Germany.
(38) Sheldrick, G. M. *SHELXTL*, Version 5.1; Siemens Analytical X-ray Systems, Inc.: Madison, WI, 1997.
(39) It should be mentioned at this point that the crystals began to lose solvent molecules immediately after isolation, recognizably becoming opaque during the data collection. It is possible, therefore, that the initial content of solvent molecules immediately after isolation could have been higher. At full occupancy of the C,O position, the formula of **I** would be $K_3AgAs_2Se_5$·0.5MeOH.

Table 1. Crystal Data and Structure Refinement Details for $K_3AgAs_2Se_5 \cdot 0.25MeOH$ (**I**), $K_2AgAs_3Se_6$ (**II**), and $Rb_2AgAs_3Se_6$ (**III**)

	I	**II**	**III**
empirical formula	$K_3AgAs_2Se_5C_{0.25}O_{0.25}H_1$	$K_2AgAs_3Se_6$	$Rb_2AgAs_3Se_6$
formula weight	777.33	884.59	977.33
temperature (K)	298	173	298
crystal system	monoclinic	monoclinic	monoclinic
space group	$P2_1/c$ (No. 14)	$P2_1/n$ (No. 14)	$P2_1/n$ (No. 14)
a (Å)	9.2286(9)	12.5994(6)	12.717(2)
b (Å)	11.508(2)	7.4980(4)	7.7329(8)
c (Å)	12.905(2)	14.2648(7)	14.368(2)
β (deg)	104.272(2)	96.625(2)	95.745(2)
V (Å^3)	1328.2(2)	1338.6(2)	1405.9(3)
Z	4	4	4
ρ_{calc} (g cm^{-3})	3.887	4.389	4.617
μ(Mo Kα) (mm^{-1})	21.053	25.752	30.808
final R indices [$I > 2\sigma(I)$][a]	$R_1 = 0.0545$, w$R_2 = 0.0982$	$R_1 = 0.0435$, w$R_2 = 0.1040$	$R_1 = 0.0393$, w$R_2 = 0.0510$
R indices (all data)[a]	$R_1 = 0.0917$, w$R_2 = 0.1075$	$R_1 = 0.0621$, w$R_2 = 0.1075$	$R_1 = 0.1003$, w$R_2 = 0.0599$

[a] $R_1 = \sum||F_o| - |F_c||/\sum|F_o|$; w$R_2 = [\sum w\{|F_o| - |F_c|\}^2/\sum w|F_o|^2]^{1/2}$, $w = 1/\sigma^2\{|F_o|\}$.

Table 2. Atomic Coordinates and Equivalent Isotropic Displacement Parameters (Å^2) for $K_3AgAs_2Se_5 \cdot 0.25MeOH$ (**I**), $K_2AgAs_3Se_6$ (**II**), and $Rb_2AgAs_3Se_6$ (**III**)

	x	y	z	U_{eq}
		Compound **I**		
K1	0.8467(4)	0.6360(3)	0.2776(3)	0.044(1)
K2	0.5364(4)	0.1962(3)	0.0778(3)	0.039(1)
K3	0.8455(4)	0.2582(3)	−0.1084(3)	0.043(1)
Ag	0.6699(1)	0.5055(1)	0.0355(1)	0.033(1)
As1	0.4892(2)	0.4223(1)	0.2444(1)	0.024(1)
As2	0.0880(2)	0.4438(1)	0.1173(1)	0.023(1)
Se1	0.6519(2)	0.4658(1)	0.4084(1)	0.028(1)
Se2	0.4816(2)	0.6011(1)	0.1489(1)	0.026(1)
Se3	0.8723(2)	0.3556(1)	0.1538(1)	0.027(1)
Se4	0.8113(2)	0.6928(1)	−0.0179(1)	0.026(1)
Se5	0.2520(2)	0.4283(1)	0.2973(1)	0.034(1)
C1/O1	0.998(8)	0.526(6)	0.462(5)	0.12(3)
		Compound **II**		
K1	0.3462(2)	−0.1125(4)	0.7610(2)	0.018(1)
K2	0.1670(2)	0.3685(4)	0.3868(2)	0.020(1)
Ag	0.1032(1)	−0.0063(2)	0.5734(1)	0.022(1)
As1	−0.1264(1)	0.0897(2)	0.6582(1)	0.012(1)
As2	0.0350(1)	−0.0562(2)	0.8696(1)	0.013(1)
As3	0.1180(1)	0.3325(2)	0.0071(1)	0.013(1)
Se1	−0.2947(1)	0.2430(2)	0.6638(1)	0.014(1)
Se2	0.0351(1)	−0.2718(2)	0.4431(1)	0.015(1)
Se3	−0.0705(1)	0.2097(2)	0.8137(1)	0.014(1)
Se4	0.0774(1)	−0.1874(2)	0.7296(1)	0.016(1)
Se5	0.2014(1)	0.0989(2)	0.9199(1)	0.015(1)
Se6	0.2952(1)	0.0860(2)	0.5396(1)	0.016(1)
		Compound **III**		
Rb1	0.3486(1)	−0.1044(1)	0.7675(1)	0.032(1)
Rb2	0.1651(1)	0.3706(1)	0.3893(1)	0.030(1)
Ag	0.1057(1)	−0.0050(1)	0.5749(1)	0.038(1)
As1	−0.1286(1)	0.0894(1)	0.6556(1)	0.021(1)
As2	0.0284(1)	−0.0415(1)	0.8685(1)	0.022(1)
As3	0.1161(1)	0.3380(1)	0.0077(1)	0.022(1)
Se1	−0.2960(1)	0.2375(1)	0.6606(1)	0.025(1)
Se2	0.0369(1)	−0.2600(1)	0.4474(1)	0.024(1)
Se3	−0.0768(1)	0.2107(1)	0.8088(1)	0.024(1)
Se4	0.0746(1)	−0.1732(1)	0.7322(1)	0.027(1)
Se5	0.1926(1)	0.1088(1)	0.9186(1)	0.025(1)
Se6	0.2976(1)	0.0814(1)	0.5412(1)	0.028(1)

the small Li^+ does not tend to incorporate in the structure. With Rb_2CO_3 as the source of the slightly more voluminous Rb^+ cation, and otherwise the same reaction conditions as for **II**, we were able to synthesize the isostructural $Rb_2AgAs_3Se_6$ (**III**). If the conditions are slightly changed, e.g. variations in the stoichiometry of the reactants, **III** is still accessible, but other phases, such as $RbAsSe_2$,[25] also arise.

Our investigations of the reaction system $AgBF_4/K_3AsSe_3$ identified several different products under systematic variation of the solventothermal conditions.[19] We could observe the formation of $K_3AgAs_2Se_5 \cdot 0.25MeOH$ and $K_2AgAs_3Se_6$ after reaction of $AgBF_4/K_3AsSe_3$ in a 1:3 ratio at 130 °C after about 2 h and 3 days, respectively. The same methanol thermal reaction for 1 week at 110 °C leads to the quaternary compound $K_5Ag_2As_3Se_9$,[20] which occasionally could also be observed as a side product of the formation of $K_2AgAs_3Se_6$. The polyanion in $K_5Ag_2As_3Se_9$ provides two different group 15/16 anions, $[As_2Se_5]^{4-}$ and $[AsSe_4]^{3-}$. The former anion contains a direct As−As bond and demands a reduction reaction, but the latter one is an oxidation product providing an As^{5+} anion. These results demonstrate in an impressive manner that, besides condensation reactions, complicated redox reactions can also occur in certain solventothermal systems. Interestingly, the same ratio of reactants in H_2O for 24 h at 110 °C produces black crystals of β-Ag_3AsSe_3,[20] which is also a kinetically stabilized product. At higher temperatures, the β-form becomes thermodynamically unstable and transforms to the α-allotrope.

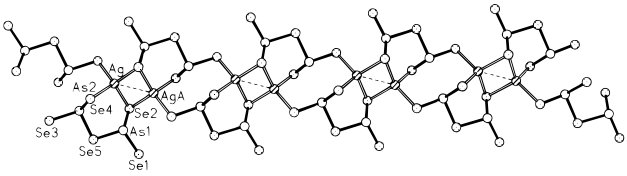

Figure 1. The $[AgAs_2Se_5]^{3-}$ chain in $K_3AgAs_2Se_5 \cdot 0.25MeOH$ (**I**). The chain contains Ψ-bitetrahedral $[As_2Se_5]^{4-}$ units and tetrahedrally coordinated Ag^+ atoms.

Structure of $K_3AgAs_2Se_5 \cdot 0.25MeOH$ (I). The anionic structure of $K_3AgAs_2Se_5 \cdot 0.25MeOH$ consists of parallel $[AgAs_2Se_5]^{3-}$ chains (Figure 1), running down the a direction of the monoclinic unit cell (Figure 2). These chains consist of ψ-bitetrahedral $[As_2Se_5]^{4-}$ units and tetrahedral coordinated Ag^+ atoms. The As−Se bond lengths of the terminal Se (As−Se_t: 2.328(2)−2.391(2) Å) atoms are, as expected, shorter than the ones of the bridging Se atom (As−Se_b: 2.446(2), 2.449(2) Å). The As−Se_b−As angle is 97.09(6)°, and the Se_t−As−Se_b angles are smaller (97.64(6)−101.82(7)°) than the Se_t−As−Se_t angles (102.32(7), 106.51(6)°). All values agree well with the ones found in other $[As_xSe_y]^{z-}$ building blocks.[15−19] The same dimeric $[As_2Se_5]^{4-}$ anion was also found in $(Me_3NH)[Ag_3As_2Se_5]$,[19] while similar $[M_2Q_5]^{4-}$ anions are present in $Sr_2Sb_2S_5 \cdot 15H_2O$,[40] $(Me_4N)_4[Sb_2Te_5]$,[41] $(CH_3NH_2)[Mn_2Sb_2S_5]$, $(HN_2(CH_2)_3NH_2)[Mn_2Sb_2S_5]$,[42] and several sulfosalts, e.g. $Tl_2MnAs_2S_5$,[43]

(40) Cordier, G.; Schäfer, H.; Schwidetzky, C. *Rev. Chim. Miner.* **1985**, *22*, 722.
(41) Warren, C. J.; Dhingra, S. S.; Ho, D. M.; Haushalter, R. C.; Bocarsly, A. B. *Inorg. Chem.* **1994**, *33*, 2709.

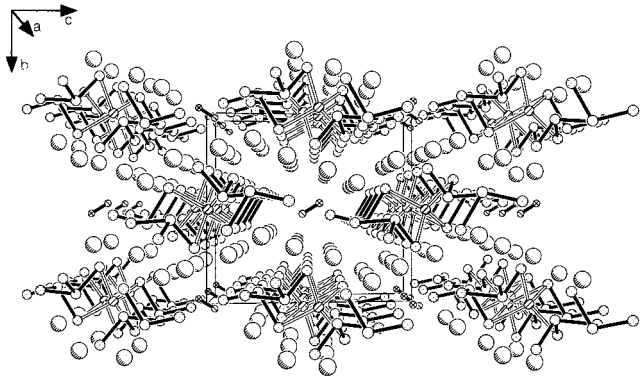

Figure 2. Unit cell of $K_3AgAs_2Se_5 \cdot 0.25MeOH$ viewed down the [100] direction.

$TlCuPbAs_2S_5$,[44] and $TlAgPbAs_2S_5$.[45] A structural isomer of $[As_2Se_5]^{4-}$ of the one discussed here, containing an As−As bond, was found in $K_5Ag_2As_3Se_9$;[19] one As atom of the As−As dumb-bell is bonded to two Se atoms, while the other one is bonded to three Se atoms, leading to a unique mixed formal oxidation state $As^{2+}-As^{4+}$ compound.

Three of the four Se_t atoms of each $[As_2Se_5]^{4-}$ group are taking part in the coordination of the Ag atoms, which reveal distorted $AgSe_4$ tetrahedral units with As−Se bond lengths between 2.696(2) and 2.761(2) Å and Se−Ag−Se angles ranging from 102.97(5) to 112.98(5)°. Because of the particular coordination mode of the $[As_2Se_5]^{4-}$ units, the Ag^+ ions exist in pairs of two, separating these units from each other. The Ag···Ag distance is 3.045(2) Å (Figure 3, dotted line). This distance is considerably longer than the single-bond metallic radius (2.68 Å),[46] as well as the Ag···Ag distance of 2.89 Å in elemental Ag.[47] Thus, no bonding $d^{10}-d^{10}$ interactions can be expected. Furthermore, the short Ag···Ag distances in **I** are rather forced by the construction of bitetrahedral Ag_2Se_6 units, leading to a central four-membered Ag_2Se_2 ring, responsible for the closer contacts. This building block is comparable to the characteristic $[M_2Q_6]^{4-}$ units of the group 14 elements (M = Si, Ge, Sn; Q = S, Se, Te), known from a large number of ternary and quaternary compounds.[48] Therefore, the structure of $K_3AgAs_2Se_5 \cdot 0.25MeOH$ can also be described as Ag_2Se_6 bitetrahedral units that are connected to $[As_2Se_5]^{4-}$ units by common Se atoms to form infinite chains of $[AgAs_2Se_5]^{3-}$. The three crystallographically different K^+ cations and one MeOH molecule lie between these chains. The MeOH molecule serves as a spacer between two neighboring $[AgAs_2Se_5]^{3-}$ chains in the *c* direction. The C/O positions are disordered, and both positions are only half-occupied. All K cations are coordinated by Se and As atoms of the $[As_2Se_5]^{4-}$ units. Only K1 is coordinated by the MeOH molecule (2.76(6) Å), together with seven Se atoms (3.373(3)−3.804(3) Å) and one As atom (3.788(3) Å), revealing a 9-fold coordination sphere. K2 and K3 are coordinated to seven/five Se and one/three As atoms, respectively, in the range 3.174(3)−3.852(4) Å, leading to an 8-fold coordination for both atoms. The shortest K···K distance between K1 and K3 is 4.170(4) Å. There are no interchain Se···Se or Se···As contacts below the van der Waals radius of 3.6 Å,[46] which therefore leads to the description of "isolated" $[AgAs_2Se_5]^{3-}$ chains.

Table 3. Bond Lengths (Å) and Angles (deg) for $K_3AgAs_2Se_5 \cdot 0.25MeOH$ (**I**), $K_2AgAs_3Se_6$ (**II**), and $Rb_2AgAs_3Se_6$ (**III**)

Bond Lengths for I			
Ag−Se4	2.696(2)	As1−Se1	2.328(2)
Ag−Se3	2.718(2)	As1−Se2	2.391(2)
Ag−Se2	2.736(2)	As1−Se5	2.449(2)
Ag−Se2A	2.761(2)	As2−Se4	2.360(2)
Ag−AgA	3.045(2)	As2−Se3	2.382(2)
		As2−Se5	2.446(2)
Selected Bond Angles for I			
Se4−Ag−Se3	110.01(5)	Se1−As1−Se2	102.32(7)
Se4−Ag−Se2	108.15(5)	Se1−As1−Se5	99.28(6)
Se3−Ag−Se2	109.70(5)	Se2−As1−Se5	101.82(7)
Se4−Ag−Se2A	102.97(5)	Se4−As2−Se3	106.51(6)
Se3−Ag−Se2A	112.98(5)	Se4−As2−Se5	103.49(7)
Se2−Ag−Se2A	112.73(5)	Se3−As2−Se5	97.64(6)
Bond Lengths for II			
Ag−Se6	2.614(2)	As1−Se3	2.422(2)
Ag−Se4	2.661(2)	As2−Se4	2.343(2)
Ag−Se2	2.711(2)	As2−Se5	2.432(2)
Ag−Se2	2.790(2)	As2−Se3	2.477(2)
Ag−AgA	3.147(2)	As3−Se6	2.328(2)
As1−Se2	2.378(2)	As3−Se1	2.441(2)
As1−Se1	2.421(2)	As3−Se5	2.454(2)
Selected Bond Angles for II			
Se6−Ag−Se4	119.66(5)	Se4−As2−Se5	100.28(7)
Se6−Ag−Se2	112.33(6)	Se4−As2−Se3	103.30(6)
Se4−Ag−Se2	109.00(6)	Se5−As2−Se3	97.05(6)
Se6−Ag−Se2A	106.61(6)	Se6−As3−Se1	105.93(6)
Se4−Ag−Se2A	97.82(5)	Se6−As3−Se5	101.25(8)
Se2−Ag−Se2A	110.22(4)	Se1−As3−Se5	97.16(6)
Se2−As1−Se1	103.56(7)	As1−Se1−As3	99.41(7)
Se2−As1−Se3	103.50(7)	As1−Se3−As2	94.86(6)
Se1−As1−Se3	87.51(6)	As2−Se5−As3	94.92(7)
		Ag−Se2−AgA	69.78(4)
Bond Lengths for III			
Ag−Se6	2.622(2)	As2−Se4	2.335(2)
Ag−Se4	2.671(2)	As2−Se5	2.434(2)
Ag−Se2	2.735(2)	As2−Se3	2.469(2)
Ag−Se2	2.772(2)	As3−Se6	2.323(2)
Ag−AgA	3.272(2)	As3−Se1	2.435(2)
As1−Se2	2.375(2)	As3−Se5	2.445(2)
As1−Se3	2.424(2)		
As1−Se1	2.424(2)		
Selected Bond Angles for III			
Se6−Ag−Se4	120.01(4)	Se4−As2−Se5	100.11(5)
Se6−Ag−Se2	113.94(4)	Se4−As2−Se3	103.06(5)
Se4−Ag−Se2	108.15(4)	Se5−As2−Se3	98.30(5)
Se6−Ag−Se2A	107.30(4)	Se6−As3−Se1	106.20(5)
Se4−Ag−Se2A	98.56(4)	Se6−As3−Se5	101.82(5)
Se2−Ag−Se2A	107.10(4)	Se1−As3−Se5	97.38(5)
Se2−As1−Se3	104.20(5)	As1−Se1−As3	100.64(5)
Se2−As1−Se1	104.10(5)	As1−Se3−As2	95.66(5)
Se3−As1−Se1	87.12(4)	Ag−Se2−AgA	72.90(4)

Structures of $K_2AgAs_3Se_6$ (II) and $Rb_2AgAs_3Se_6$ (III). These two isostructural compounds possess the 2D anion $[AgAs_3Se_6]^{2-}$ (Figure 4). The $[AsSe_2]^-$ chains in this anion can be recognized (Figure 5a), as a product of infinite condensation of $[AsSe_3]^{3-}$ pyramidal building units (eq 6). The As−Se_b distances are again significantly longer (**II**, 2.422(3)−2.476(2) Å; **III**, 2.424(2)−2.469(2) Å) than the As−Se_t distances (**II**,

(42) Bensch, W.; Schur, M. *Eur. J. Solid State Inorg. Chem.* **1996**, *33*, 1149.
(43) Gostojic, M.; Edenharter, A.; Nowacki, W.; Engel, P. *Z. Kristallogr.* **1982**, *158*, 43.
(44) Takeuchi, Y.; Ohmasa, M.; Nowacki, W. *Z. Kristallogr.* **1968**, *127*, 349.
(45) Marumo, E.; Nowacki, W. *Z. Kristallogr.* **1967**, *125*, 249.
(46) Pauling, L. *The Nature of the Chemical Bond*, 3rd ed.; Cornell University Press: Ithaca, NY, 1960.
(47) (a) Jansen, M. *Angew. Chem., Int. Ed. Engl.* **1987**, *26*, 1098. (b) Straumanis, M. E. *Monatsh. Chem.* **1971**, *102*, 1377.
(48) See, for example: (a) Krebs, B.; Pohl, S. *Z. Anorg. Allg. Chem.* **1972**, *393*, 241. (b) Li, J.; Marler, B.; Kessler, H.; Soulard, M.; Kallus, S. *Inorg. Chem.* **1997**, *36*, 4697. (c) Eisenmann, B.; Hansa, J. *Z. Kristallogr.* **1993**, *203*, 299. (d) Sheldrick, W. S.; Schaaf, B. *Z. Anorg. Allg. Chem.* **1994**, *620*, 1041. (e) Reference 1a.

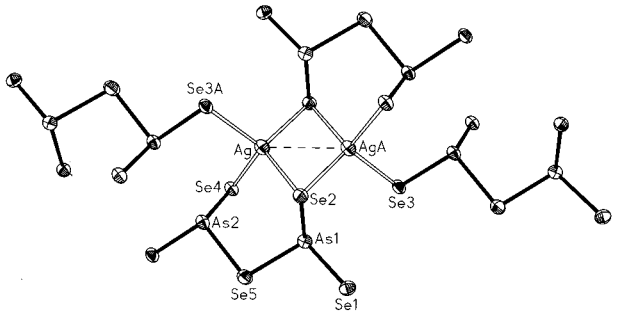

Figure 3. The bitetrahedral Ag_2Se_6 unit of the $[AgAs_2Se_5]^{3-}$ chains in **I** with a central planar Ag_2Se_2 ring (50% thermal vibrational ellipsoids).

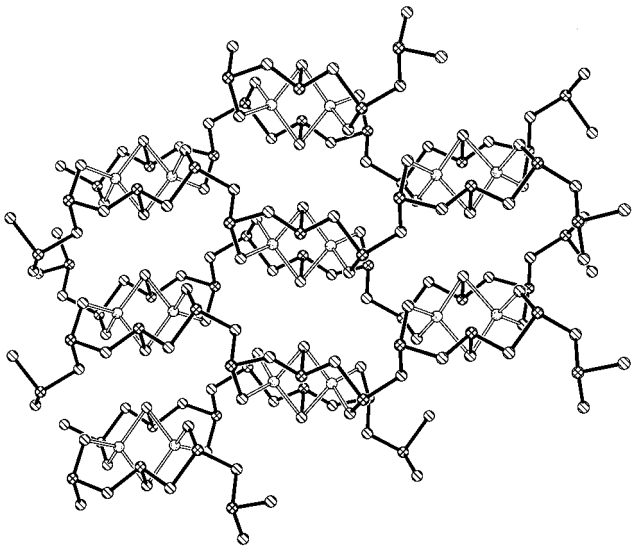

Figure 4. The $[AgAs_3Se_6]^{2-}$ layers of **II** and **III** viewed approximately from [101] direction. The manner in which the undulated $[AsSe_2]^-$ chains are coordinating to the Ag^+ atoms leads to huge holes able to capture the K^+ and Rb^+ cations for **II** and **III**, respectively.

2.329(2)−2.376(2) Å; **III**, 2.323(2)−2.375(2) Å). The same kind of chains exist in the ternary $AAsSe_2$ compounds with A = Na[49] or K, Rb, Cs,[25] and their As−Se bond length ranges agree well with the values found in **II** and **III**. All Se−As−Se and As−Se−As angles lie within the expected range (see Table 3). However, the $[AsSe_2]^-$ chains in **II** and **III** show a remarkable undulation, as can be manifested by their torsion angles. The chain conformation repeats after a sequence of six As atoms. Therefore, it can be classified as a "sechser" single chain, according to the nomenclature proposed by Liebau.[50] In contrast, the different $AAsSe_2$ compounds with A = Na, K, Rb, Cs have periodicities of 2 or 4. Table 4 shows the torsion angle sequences for $K_2AgAs_3Se_6$ and $Rb_2AgAs_3Se_6$ within the repeating unit. The scatter of the values is an indicator for the degree of undulation. Figure 5a shows this undulation of the chains, changing also their main directory at every fourth As atom.

The Ag^+ ions are coordinated by two $[AsSe_2]^-$ chains to form sheets of the composition $[AgAs_3Se_6]^{2-}$ (Figure 4). The result is a double sheet of $[AsSe_2]^-$ chains with tetrahedrally coordinated Ag atoms in the inner part of the thick layers (Figure 6). Only the terminal Se atoms of the $[AsSe_2]^-$ chains take part in the Ag^+ coordination, exhibiting Ag−Se bond distances of 2.615(2)−2.790(2) Å for **II** and 2.622(1)−2.772(1) Å for **III**. It is important to note that, similar to the case of **I**, the Ag^+ atoms in these two compounds are also arranged in pairs of two, since again Ag_2Se_6 bitetrahedral units with a central rhombic, four-membered Ag_2Se_2 ring are present. The Ag··· Ag distances are 3.147(2) Å in **II** and 3.272(2) Å in **III**, slightly longer than those in **I**.

Another appropriate description of this structure type is to view it as assembled by the condensation of $[Ag_2As_6Se_{14}]^{8-}$ cores (Figure 5b) through common Se atoms to form the

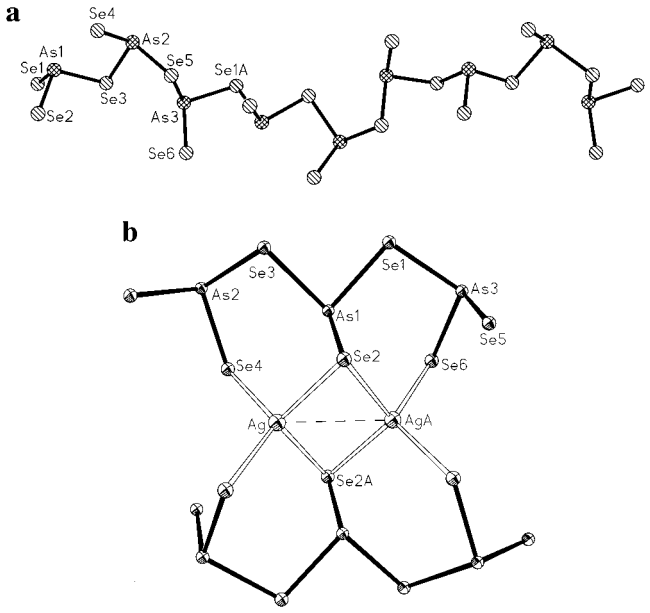

Figure 5. (a) An undulated $[AsSe_2]^-$ chain as part of the anionic structures of $K_2AgAs_3Se_6$ (**II**) and $Rb_2AgAs_3Se_6$ (**III**). The chain direction changes every fourth As atom. (b) Structure of **II**/**III** also described as built up of large $[Ag_2As_6Se_{14}]^{8-}$ clusters, which condense by sharing Se atoms to form the $[AgAs_3Se_6]^{2-}$ sheet anion (50% thermal vibrational ellipsoids).

Table 4. Torsion Angles of the $[AsSe_2]^-$ Chains of $K_2AgAs_3Se_6$ (**II**) and $Rb_2AgAs_3Se_6$ (**III**)[a]

	II	III
Se1−As1−Se3−As2[b]	+144.9(1)	+144.9(1)
As1−Se3−As2−Se5	+126.5(1)	+126.5(1)
Se3−As2−Se5−As3	+47.5(1)	+49.4(1)
As2−Se5−As3−Se1A	+115.8(1)	+116.4(1)
Se5−As3−Se1A−As1A	+82.6(1)	+84.5(1)
As3−Se1A−As1A−Se3	+177.3(1)	+177.8(1)
Se1A−As1A−Se3A−As2A[b]	−144.9(1)	−144.9(1)

[a] Identity within the chain is reached after every six As atoms; therefore, they can be classified as "sechser" single chains. [b] The sign of the angles is inverted after each series of atoms.

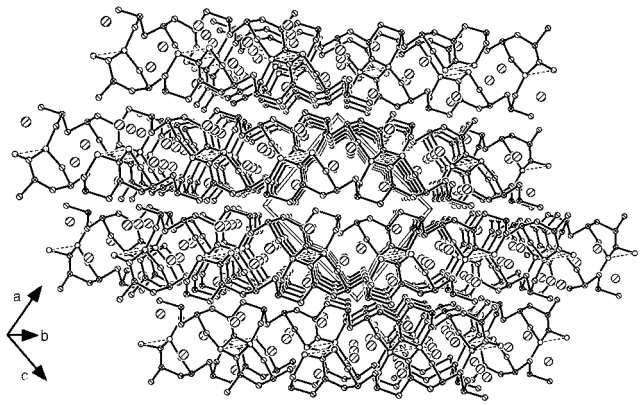

Figure 6. Unit cell of **II**/**III** viewed from the [010] direction. The thickness of one $[AgAs_3Se_6]^{2-}$ layer anion is about 10 Å.

(49) Eisenmann, B.; Schäfer, H. *Z. Anorg. Allg. Chem.* **1979**, *456*, 87.
(50) Liebau, F. *Naturwissenschaften* **1962**, *49*, 41.

$[AgAs_3Se_6]^{2-}$ sheets. Whereas the terminal atoms Se4 and Se6 are coordinating to one of the Ag atoms of an Ag−Ag pair, the middle Se2 atom, taking part in the formation of the Ag_2Se_2 ring, is coordinating both. This coordination scheme leads to slightly distorted tetrahedral coordinated Ag atoms (**II**, 97.83(5)−119.65(5)°; **III**, 98.56(4)−120.01(4)°). The advantage of this alternative description is a much easier understanding of the formation of large cavities within the sheets (Figures 4 and 6), since the condensation of the huge $[Ag_2As_6Se_{14}]^{8-}$ clusters can most probably not lead to a dense sheet. Unlike most other two-dimensional structures in this class of compounds, the cations are now located *within* the sheets rather than between them. It is interesting to note that there are no substantial differences in cavity diameters for **II** and **III**; the closest contacts between two clusters in the *b* direction are 3.932 and 4.151 Å for **II** and **III**, respectively (see Figure 4). However, in the direction of the $[AsSe_2]^-$ chains, where the cavities have their longest expansions, the difference is negligible (**II**, 13.838 Å; **III**, 13.907 Å). An important factor for achieving such cavity diameters within these sheets may be the high flexibility of the $[AsSe_2]^-$ chains. The chain flexibility is evident in the structures of the various $AAsSe_2$ compounds, e.g. A = Na^+,[49] K^+, Rb^+, Cs^+.[25] In these systems, the $[AsSe_2]^-$ chains possess different conformations to generate the "right" space for the respective cations.

The alkali metal cations A1 (A = K, Rb) are 7-fold coordinated by Se atoms (K1, 3.328(3)−3.483(3) Å; Rb1, 3.473(2)−3.555(2) Å), whereas the A2 atoms have a 9-fold coordination environment with eight Se atoms and one As atom taking part (K2, 3.315(3)−3.786(4); Rb2, 3.432(2)−3.746(2) Å). In both cases, the coordination polyhedra are very irregular. Both K1 and Rb1 are coordinated only by atoms within the same sheet, whereas K2 and Rb2 have two coordinating Se atoms of a neighboring sheet. There are several long Se···As and Se···Se contacts as a result of the interactions between neighboring sheets starting at 3.36 Å (contact Se1···As2 in **II**; 3.40 Å in **III**), which is significantly shorter than the Se−As van der Waals distance of 3.6 Å.[46]

Properties. The thermal behavior of **I**−**III** was investigated by differential thermal analysis (DTA) in the range 50−400 °C. $K_2AgAs_3Se_6$ and $Rb_2AgAs_3Se_6$ have very similar melting points: 271.5 and 283.6 °C (Figure 7b,c), respectively; that of $K_3AgAs_2Se_5$·0.25MeOH is slightly lower at 259.1 °C (Figure 7a). The thermal gravimetric analysis of the last compound showed that it starts to lose its MeOH slightly above room temperature (∼40 °C). None of the compounds have any transitions upon cooling, consistent with an incongruent melting point. A second heating/cooling cycle for all three compounds showed no transitions up to 400 °C, and the X-ray powder patterns of the residues were amorphous. This is in agreement with the proposal that these compounds are kinetically stabilized products which decompose at higher temperatures and are therefore, probably, not accessible via classical high-temperature direct combination reactions. For example, the reactions of $K_2Se/Ag/As_2Se_3/Se$ or $K_2Se/Ag/As/Se$ in the stoichiometric ratio for $K_2AgAs_3Se_6$ at 500 °C produces only amorphous black powders, as verified by powder X-ray diffraction.

A representative optical transmission spectrum collected from a single crystal of $K_2AgAs_3Se_6$ is shown in Figure 8. The band gap was determined, after conversion to absorption data, from extrapolation of the data along the absorption edge and found to be 2.07 eV. A similar band gap could be determined from reflection data of the pulverized samples. The value for $Rb_2AgAs_3Se_6$ is slightly lower (1.95 eV), whereas $K_3AgAs_2Se_5$·0.25MeOH has a comparable value of 2.10 eV. The presence of optical gaps and the electron-precise nature of the compounds confirm that we are dealing with typical wide band gap semiconductors.

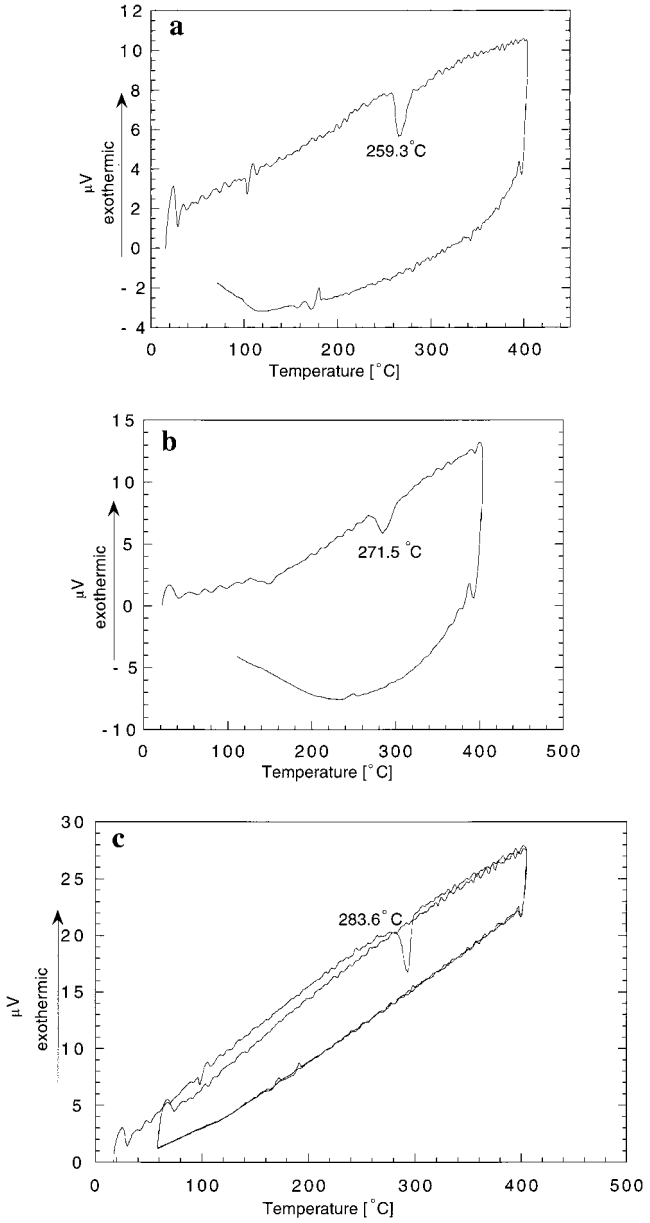

Figure 7. DTA diagram of (a) $K_3AgAs_2Se_5$·0.25MeOH (**I**), (b) $K_2AgAs_3Se_6$ (**II**), and (c) $Rb_2AgAs_3Se_6$ (**III**) (heating/cooling rate 5 °C/min).

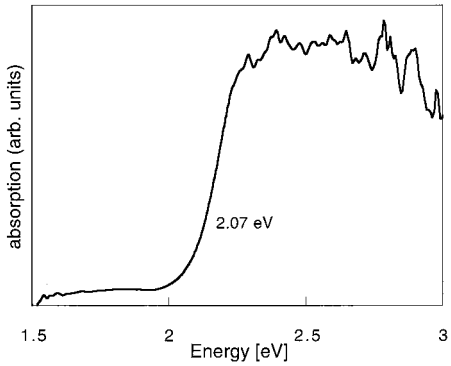

Figure 8. Single-crystal UV/vis spectrum of $K_2AgAs_3Se_6$ (**II**).

The Raman spectra of well-grown single crystals of all three compounds were recorded between 75 and 2500 cm^{-1}. K_3-

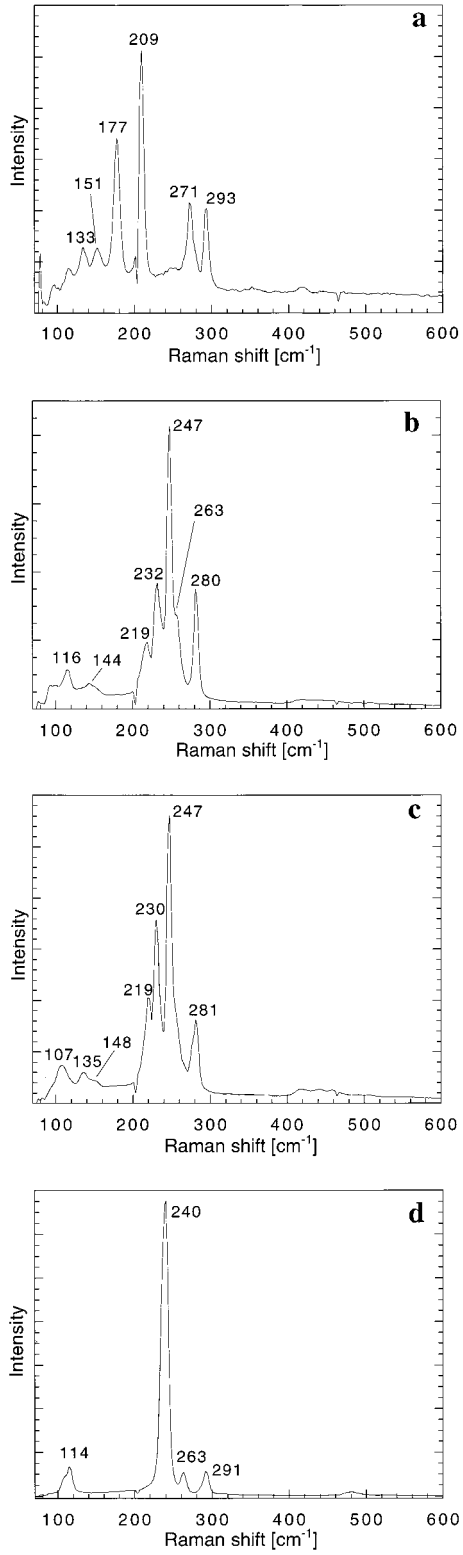

Figure 9. Raman spectra of single crystals of (a) $K_3AgAs_2Se_5 \cdot 0.25MeOH$ (**I**), (b) $K_2AgAs_3Se_6$ (**II**), (c) $Rb_2AgAs_3Se_6$ (**III**), and (d) $RbAsSe_2$.[25]

$AgAs_2Se_5 \cdot 0.25MeOH$ shows a number of peaks between 100 and 300 cm^{-1}, with two strong peaks at 177 and 209 cm^{-1} and two weaker ones at 271 and 293 cm^{-1} (Figure 9a). In this region, As−Se vibrations from the $[As_2Se_5]^{4-}$ anion can be expected. To verify the existence of the $[AsSe_2]^-$ chains in **II** and **III**, we also recorded the Raman spectrum of $RbAsSe_2$. The latter compound was first reported by Sheldrick et al.[25] and reveals $[AsSe_2]^-$ chains. With reaction conditions different from the ones used for the synthesis of $Rb_2AgAs_3Se_6$, we occasionally obtained single crystals of this compound while aiming to synthesize other quaternary Rb/Ag/As/Se phases.

Figure 9b−d shows the Raman spectra of **II**, **III**, and $RbAsSe_2$. It shows a strong peak at 240 cm^{-1} and three weaker ones at 263, 291, and 114 cm^{-1}. $K_2AgAs_3Se_6$ and $Rb_2AgAs_3Se_6$ have their strongest frequencies at 247 cm^{-1}. The other three peaks which could be observed are also found to be comparable; the peak at 280 cm^{-1} is now stronger for **II** and **III**, whereas the one at 263 cm^{-1} is only a shoulder of the strong peak at 247 cm^{-1} (stronger for the K compound; see Figure 9b,c). The slight shift in the peaks, as well as the variations in intensities, is probably due to the covalent interactions of the $[AsSe_2]^-$ chains with the Ag^+ atoms in **II** and **III**, whereas they exist as "free" chains in $RbAsSe_2$. Additional peaks appear at 219 and 232 cm^{-1} for **II** and 219 and 230 cm^{-1} for **III**, together with some weak and broad intensity peaks between 80 and 170 cm^{-1}. The former peaks can most probably be assigned to Ag−Se vibration modes. The absorptions at lower frequencies may result from collective lattice modes or other vibrations associated with the alkali metal cations.

Concluding Remarks

The three new quaternary compounds $K_3AgAs_2Se_5 \cdot 0.25MeOH$ (**I**), $K_2AgAs_3Se_6$ (**II**), and $Rb_2AgAs_3Se_6$ (**III**) adopt new structure types and are accessible only solventothermally. The outcome of the reaction of **I** and **II** in a reaction of K_3AsSe_3 with $AgBF_4$ is strongly dependent on the reaction time (and temperature). A higher degree of condensation of the $[AsSe_3]^{3-}$ units can be observed in the products for longer reaction times. The $[As_2Se_5]^{4-}$ unit in **I** is a one-step condensation of two such units (eq 1), but prolonged reaction times lead to infinite condensation into $[AsSe_2]^-$ chains in **II** and **III**. A similar trend of oligomeric condensation for short reaction times can also be observed in the Rb system, but due to the different nature of the products, these results will be reported elsewhere.[51] The presence of these building units can be identified by Raman spectroscopy. The high negative charge of the polyanion $[AgAs_2Se_5]^{3-}$ in **I** is responsible for their complete separation from each other by the K^+ cations in the crystal structure. On the other hand, the $[AgAs_3Se_6]^{2-}$ sheets in **II** and **III** provide large cavities for the K^+ or Rb^+ cations. The possibility to adopt both K^+ and Rb^+ cations in the same structure type mirrors the high flexibility of the network, which is mainly due to the relatively floppy $[AsSe_2]^-$ chains within the polyanion. As a consequence, short Se···As contacts below the van der Waals radius can be observed between neighboring sheets.

Acknowledgment. Support from the National Science Foundation (Grant CHE 96-33798, Chemistry Research Group) and the Petroleum Research Fund, administered by the American Chemical Society, is gratefully acknowledged. We also acknowledge the use of the W. M. Keck Microfabrication Facility at Michigan State University, an NSF MRSEC facility. Part of this work was carried out using the facilities of the Center for Electron Optics of Michigan State University. M.W. thanks the Deutsche Forschungsgemeinschaft for a postdoctoral research fellowship.

Supporting Information Available: Tables of crystal data and structure refinement details, positional and thermal parameters of all atoms, and bond distances and angles for **I**−**III**. This material is available free of charge via the Internet at http://pubs.acs.org.

IC990274R

(51) Wachhold, M.; Kanatzidis, M. G. *Inorg. Chem.*, in press.